Available online at www.sciencedirect.com
SCIENCE DIRECT®
Journal of Membrane Science 241 (2004) 143–160
journal of MEMBRANE SCIENCE
www.elsevier.com/locate/memsci

Nanofiltration of natural organic matter with H_2O_2/UV pretreatment: fouling mitigation and membrane surface characterization

Wonho Song [a], Varadarajan Ravindran [a], Bruce E. Koel [b], Massoud Pirbazari [c,*]

[a] *Environmental Engineering Program, Department of Civil Engineering, University of Southern California, Los Angeles, CA 90089, USA*
[b] *Department of Chemistry, University of Southern California, Los Angeles, CA 90089, USA*
[c] *Department of Civil and Environmental Engineering, University of Southern California, Los Angeles, CA 90089, USA*

Received 1 August 2003; received in revised form 21 April 2004; accepted 26 April 2004

Abstract

This research investigated the application of H_2O_2/UV oxidation for source water pretreatment, and membrane cleaning to improve the performance of nanofiltration processes. It further examined the nature and mechanisms of membrane fouling by natural organic matter (NOM), and membrane cleaning using different chemical agents, by employing several surface characterization techniques. These techniques included attenuated total reflection-Fourier transform infrared spectroscopy (ATR-FTIR), X-ray photoelectron spectroscopy (XPS), atomic force microscopy (AFM), and scanning electron microscopy (SEM). The study revealed that significant improvement could be achieved in the efficiency and economics of nanofiltration for removing NOM and synthetic organic chemicals (SOCs) by employing source water pretreatment and membrane cleaning strategies. The H_2O_2/UV oxidation of source water prior to nanofiltration showed potential for the following: (i) mitigation of flux decline due to membrane fouling, (ii) removal of the pesticide alachlor and hydrogen sulfide, and (iii) improvement in membrane cleanability. Nonetheless, careful control of the preoxidation conditions was exercised to arrive at a reasonable compromise between fouling mitigation and NOM rejection.

Keywords: Nanofiltration; Membrane fouling; Surface characterization; Hydrogen peroxide; Ultraviolet radiation; Natural organic matter; Advanced oxidation

1. Introduction

Membrane technologies can be competitive in terms of efficiency and economics for water treatment applications, owing to their ability to remove a broad spectrum of organic and inorganic contaminants and pathogenic microorganisms. However, a factor that significantly affects their overall performance and economics is permeate flux deterioration caused by restricted membrane transport due to fouling problems. Membrane fouling due to natural organic matter (NOM), exemplified by humic substances, polysaccharides, and proteins, is a major cause for flux decline [1–3]. Therefore, this article addresses certain important aspects of controlling permeate flux decline, namely, source water pretreatment for destruction or transformation of NOM, and membrane cleaning for flux recovery.

Prior to the use of membrane processes in water treatment applications, coagulation/flocculation, ozonation, and carbon adsorption processes were generally employed for pretreatment of source waters, especially those containing NOM [3,4]. However, it must be noted that conventional coagulation/flocculation processes might not eliminate a

Abbreviations: AFM, atomic force microscopy; ATR-FTIR, attenuated total reflection-Fourier transform infrared spectroscopy; DOC, dissolved organic carbon; MCL, maximum contaminant level; MWCO, molecular weight cutoff; NOM, natural organic matter; OCWD, Orange County Water District; PMCL, proposed maximum contaminant level; SDS, sodium dodecyl sulfate; SEM, scanning electron microscopy; SOCs, synthetic organic chemicals; SUVA, specific ultraviolet absorbance; $SUVA_{254}$, specific ultraviolet absorbance at 254 nm; $SUVA_{310}$, specific ultraviolet absorbance at 310 nm; TDS, total dissolved solids; THMFP, trihalomethane formation potential; THMs, trihalomethanes; TOC, total organic carbon; UVA_{254}, ultraviolet absorbance at 254 nm; UVA_{310}, ultraviolet absorbance at 310 nm; XPS, X-ray photoelectron spectroscopy

* Corresponding author. Tel.: +1 213 740 0592; fax: +1 213 744 1426.
E-mail address: pirbazar@usc.edu (M. Pirbazari).

0376-7388/$ – see front matter © 2004 Elsevier B.V. All rights reserved.
doi:10.1016/j.memsci.2004.04.034

significant fraction of NOM. A comparative study by Crozes et al. [5] showed that ozonation was more effective than activated carbon adsorption in minimizing flux decline attributed to adsorptive membrane fouling by dextran and tannic acid, compounds that serve as surrogates for certain components of NOM. The H_2O_2/UV oxidation process has shown potential for complete destruction of synthetic organic chemicals (SOCs), and transformation of humic or hydrophobic substances into non-humic or less hydrophobic components. In this regard, H_2O_2/UV oxidation pretreatment simultaneously confers a twofold advantage: (i) mitigation of flux decline due to NOM fouling and (ii) removal of contaminants such as SOCs and hydrogen sulfide. Additionally, the non-selective reactivity of hydroxyl radical vis-à-vis molecular ozone during pretreatment might reduce the formation of undesirable non-humic substances, such as polysaccharides and biodegradable oxidation byproducts. Furthermore, UV irradiation and residual hydrogen peroxide, as well as generated hydroxyl radicals, could significantly mitigate membrane fouling. Nonetheless, pretreatment of source water could slow down but not entirely eliminate membrane fouling. Effective chemical cleaning would therefore be necessary to detach different classes of foulants from the membrane and restore its permeate flux characteristics [6,7]. Furthermore, selection of appropriate chemical cleaning agents might be critical because incompatible combinations of cleaning agent and membrane material could lead to irreversible flux loss, poor solute rejection, unnecessary costs through excessive chemical use, and/or reduction in membrane life spans [7,8].

This paper discusses the applications of H_2O_2/UV oxidation pretreatment and membrane cleaning strategies for improving the performances of nanofiltration processes. The NOM-containing groundwater obtained from a deep aquifer in southern California was used as feed for laboratory-scale crossflow membrane experiments. The decompositions of NOM, SOCs (exemplified by the pesticide alachlor), and hydrogen sulfide during H_2O_2/UV oxidation were investigated. The primary objective was to evaluate the impact of H_2O_2/UV preoxidation and associated process conditions on nanofiltration performance with reference to permeate flux, permeate quality, and membrane cleanability for flux recovery. Correlations were established between the performances of virgin, fouled, and cleaned membranes, and their surface properties, based on these analytical surface characterization techniques: attenuated total reflection-Fourier transform infrared spectroscopy (ATR-FTIR), X-ray photoelectron spectroscopy (XPS), atomic force microscopy (AFM), and scanning electron microscopy (SEM). These surface characterization techniques provided insight into the mechanistic features associated with membrane fouling due to NOM, pretreatment of source water by H_2O_2/UV oxidation, and membrane cleaning using different strategies.

2. Background

2.1. Pretreatment by H_2O_2/UV oxidation and nanofiltration performance

Advanced oxidation processes employing ozone, hydrogen peroxide, UV radiation, photo-catalysis, or any combinations thereof, can alter the functional groups composition, molecular structure, molecular weight distributions, and physico-chemical as well as biological characteristics of NOM, and therefore affect subsequent water treatment processes. Such oxidative processes can have two major effects on NOM molecules: (i) minor alterations in functional groups without major breakdown of macromolecular systems, and (ii) major breakdown of large aromatic moieties into micromolecular compounds such as aliphatic organic acids. These two effects could influence membrane processes, either favorably or unfavorably, from the standpoints of fouling, cleanability, and rejection characteristics. In evaluating the effects of minor changes in the functional groups on adsorptive organic fouling, the following actors should be considered: (i) physical sorption of organic molecules on membrane surface, (ii) electrostatic interactions between those organics and the membrane, and (iii) chemical interactions between the membrane and NOM molecules.

Physical sorption of NOM molecules on the surface can be attributed to van der Waals forces, and is therefore relatively weak. Electrostatic interactions between NOM and membrane surface are often related to their polar functional groups (such as carboxylic, phenolic, and amidic groups). Chemical interactions between NOM molecules and membrane surface are generally stronger than physical sorption or electrostatic interactions. For instance, the phenolic and peptide groups in humic acid can form hydrogen bonds with carbonyl or polyamide groups on the membrane fabricated from a cross-linked aromatic polyamide, as shown in Fig. 1 [9]. Additionally, the peptide bonds can also form hydrogen bonds with phenolic groups of other NOM molecules, thereby increasing the apparent molecular sizes. The hydrogen bonds are characterized by high dissociation energies of 5–10 kcal/mol as compared to electrostatic bonds characterized by low energies of 2–3 kcal/mol [10], and may cause severe organic fouling. However, upon H_2O_2/UV oxidation, the phenolic groups in aromatic moieties of NOM undergo transformation to quinone groups [11,12], as illustrated in Fig. 1. These quinone groups have a low propensity for hydrogen bonding with carbonyl and amide groups on the membrane surface, but predominantly form hydrogen bonds with water molecules [2,9]. Furthermore, the generated quinone groups do not form hydrogen bonds with the peptide moiety of another NOM molecule, a factor that precludes multi-layer sorption because the NOM molecules may not effectively compete with water molecules for the quinone sites associated with the first NOM layer sorbed on the membrane.

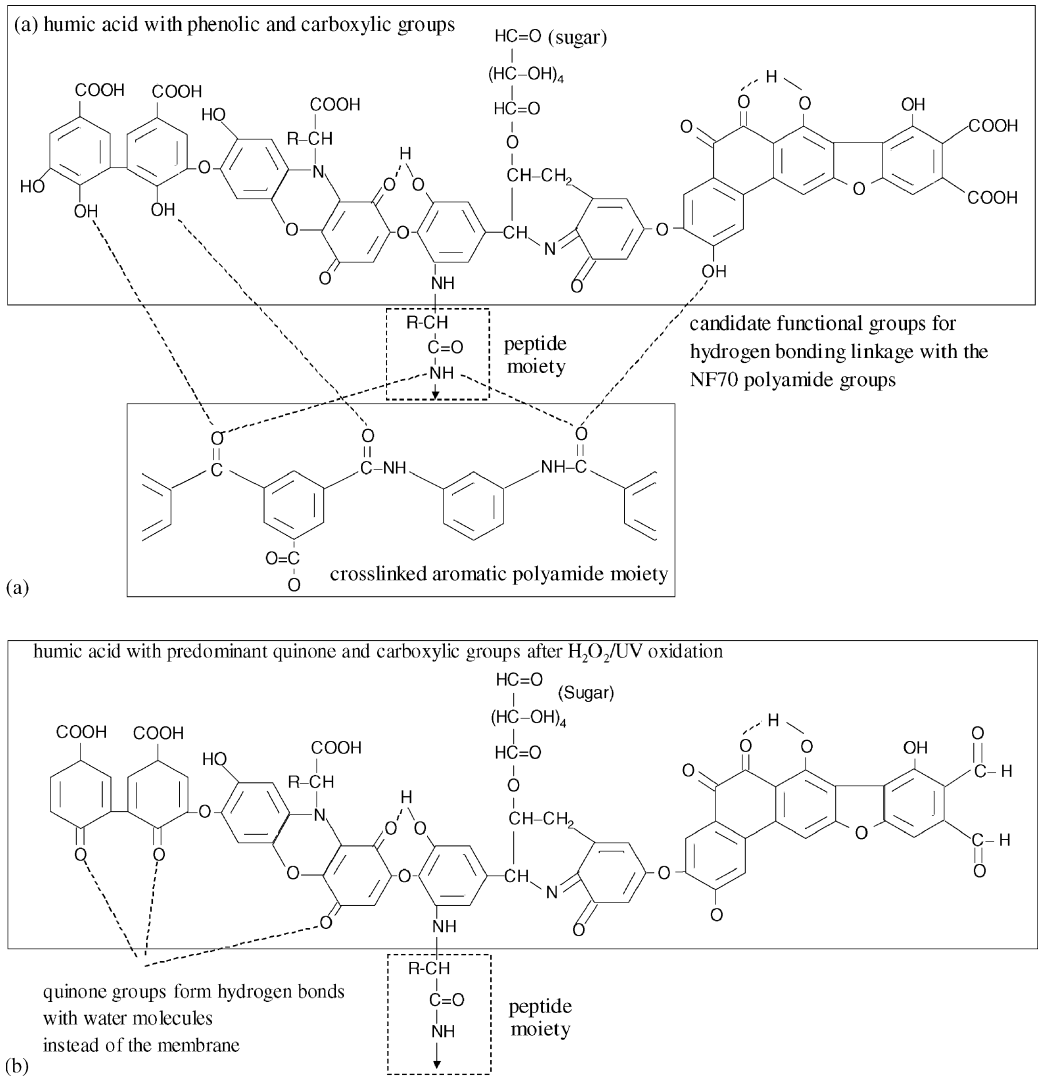

Fig. 1. Surface interactions between humic acid and the NF70 membrane: (a) before and (b) after preoxidation of NOM (minor alteration in functional groups without major breakdown of macromolecules).

Potential flux enhancement could be experienced due to major breakdown of NOM macromolecules by advanced oxidation processes. Indicators for breakdown include decreases in relative amount of humic, aromatic and resin-retained fractions [2,13,14]. Transformation of NOM by ozonation was investigated by Edwards and Benjamin [15] who identified and quantified the reaction products. They observed the destruction of carbon-carbon double bonds, and the production of simple organic acids and aldehydes. After surveying for 27 simple organic acids, they noted that oxalic acid was the dominant product with substantial generation of acetic, lactic and formic acids, and traces of gallic, phthalic, fumaric, malonic, valeric and glycolic acids.

Contemporaneously, Backlund [12] investigated the NOM decomposition in lake water under UV and H_2O_2/UV oxidations, and identified as well as quantified the reaction products in each case. The investigator noted that the major products in these processes were oxalic, acetic, malonic, and *n*-butanoic acids, and the minor products were propanoic, hexanoic and butanedioic acids. Backlund further observed that the combination of hydrogen peroxide and UV radiation yielded substantially higher amounts of organic acids than UV radiation alone. Although the major organic acids accounted for only 20% of the dissolved organic carbon (DOC) for the UV oxidation, they accounted for nearly 80% of the DOC for the H_2O_2/UV oxidation [12]. These organic acids, based on their molecular sizes, could lead to some surface fouling in nanofiltration or reverse osmosis membranes, but might potentially cause more internal pore fouling in ultrafiltration or microfiltration membranes. This could be attributed to the ability of nanofiltration or reverse osmosis membranes to retain the NOM molecules causing more surface fouling; while ultrafiltration and microfiltration membranes would facilitate their passage and increase the possibility of pore sorption and internal fouling.

Additionally, these organic acids would react with alkaline solutions, and could therefore be easily removed from the membrane surface by caustic cleaning (vis-à-vis acid cleaning or surfactant cleaning) for permeate flux recovery. However, as these organic acids were easily biodegradable, they constituted ideal substrates for microbial growth, a factor that could contribute to biological fouling and deterioration in permeate quality. Therefore, H_2O_2/UV oxidation could cause increased biological fouling although it could possibly reduce organic fouling. Nonetheless, biological fouling could also be reduced by preoxidation due to the antibiotic effects of UV radiation and hydrogen peroxide.

2.2. Membrane foulants and their characterization

A rigorous characterization of membranes could provide necessary information on the nature of foulants and their associated fouling mechanisms. For example, an FTIR spectroscopy of membranes at different incident angles demonstrated that internal pore adsorption is mainly responsible for fouling in ultrafiltration membranes [16], consistent with the results of preferential NOM adsorption onto internal pore surfaces obtained by Jucker and Clark [17]. The streaming potential, contact angle, and XPS measurements were used by Jucker and Clark [17] to investigate the mechanisms for adsorptive fouling by humic substances under the influence of calcium ions and different pH conditions. Her et al. [18] used the FTIR, X-ray diffraction, X-ray fluorescence, and SEM techniques to study precipitation scaling attributed to inorganics such as calcium carbonate and calcium sulfate. These researchers further observed that heterogeneous crystallization of inorganic and organic deposits caused more significant flux decline than homogeneous crystallization of inorganic deposits alone, consistent with the earlier findings of Schäfer et al. [13].

3. Materials and Methodologies

3.1. Materials

3.1.1. Source water

Groundwater obtained from the Orange County Water District (OCWD) was used in the H_2O_2/UV oxidation and nanofiltration studies. The water quality characteristics included high color (80–110 color units), low total dissolved solid (TDS) concentrations (235–250 mg/L), and a nearly constant pH value of ~8 due to carbonate species (Table 1). The groundwater color is mainly attributed to naturally occurring humic substances, as suggested by the high value of 0.05–0.06 mg^{-1} L cm^{-1} for specific ultraviolet absorbance at 254 nm ($SUVA_{254}$).

3.1.2. UV lamps

Low intensity and low-pressure mercury vapor lamps (American Ultraviolet Company, Murray Hill, NJ) of power ratings 8 and 16 W were used as light sources. Typically, about 99% of energy emitted from these lamps was at a wavelength of 254 nm. The light intensities at 254 nm were measured periodically to detect any deterioration in its performance. The UV radiation intensities (I_0) for the 16 and 8 W lamps were estimated as 1.8 and 2.4 × 10^{-6} einstein/L s, respectively, using hydrogen peroxide actinometry as described by Linden and Darby [19].

Table 1
Characteristics of groundwater from a deep well of OCWD

Constituent	Concentration[a]
pH	7.9–8.4
Conductivity (μS/cm)	340–370
TDS (mg/L)	235–250
Color (Pt–Co)	80–110
Turbidity (NTU)	<1
TOC (mg/L)	3.5–4.0
UVA_{254}	0.19–0.22
THMs (μg/L, 20 °C, 24 h)	280–320
Dissolved sulfide (μg/L as S^{2-})	550–590
$C_{T,CO3}$ (mM)	2.8–3.1
Fluoride (mg/L)	0.7–0.9
Chloride (mg/L)	12–15
Sodium (mg/L)	84[b]
Potassium (mg/L)	0.8[b]
Magnesium (mg/L)	1.1[b]
Calcium (mg/L)	8.1[b]
Ammonia-N (mg/L)	0.4[b]
Sulfate (mg/L)	10[b]

[a] Obtained from this work.
[b] Reported by OCWD Colored Water Hydrology Department (1996).

3.1.3. Membrane

This study employed a commercially available thin-film composite NF70 nanofiltration membrane (FilmTec Corporation, Dow Chemical Co., Midland, MI), made of a cross-linked aromatic polyamide with a polysulfone porous support, whose characteristics are shown in Table 2. The membranes originally provided as spiral-wound modules, were unrolled as flat sheets, and stored in deionized (DI) water at 20 °C prior to use in the laboratory-scale plate-and-frame membrane cell operated in the crossflow mode.

Table 2
Characteristics of the NF70 membrane

Properties	Value
Skin layer material	Cross-linked aromatic polyamide
Maximum operating pressure	250 psig (1700 kPa)[a]
Recommended operating pressure	70 psig[a]
pH range (continuous operation)	3–9[a]
pH range (short-term cleaning)	1–11[a]
Maximum operating temperature	35 °C[a]
Maximum feed silt density index	SDI 5[a]
Molecular weight cut off	200–250 Da[b]
Contact angle	27° (clean membrane)[b]
surface charge (at pH of 6–9)	−22 to −33 mV[b]

[a] Nominal value reported by the manufacturer.
[b] Tu et al. [9].

3.1.4. Analytical techniques

The UV absorbances of aqueous samples at wavelengths of 254 and 310 nm designated as UVA_{254} and UVA_{310} were measured by a Lamda 4A UV-Visible spectrophotometer (Perkin Elmer, Norwalk, CT). The total organic carbon (TOC) concentrations were measured using a Shimadzu TOC-5000 analyzer (Shimadzu Scientific Instruments, Columbia, MD). The $SUVA_{254}$ or $SUVA_{310}$ values were obtained from the ratio of UVA_{254} or UVA_{310} to TOC. The color of water samples was measured by spectrophotometry at 455 nm against standardized platinum–cobalt (Pt–Co) reference solutions.

The hydrogen peroxide concentrations at low ranges (≤10 mM) were determined by a cobalt-UV spectrometry method [20], and at high concentrations (70–100 mM) by titration against potassium permanganate [21].

The 24 h trihalomethane formation potential (THMFP) was determined by the uniform formation conditions test discussed by Summers et al. [22]. In this technique, the water samples were chlorinated (at a Cl_2/TOC ratio of approximately 3 mg/mg) and incubated for 24 h at a pH of 8.0 and temperature of 20 °C, maintaining a minimum chlorine residual of 1.0 mg/L. The trihalomethanes (THMs) from aqueous samples were extracted by liquid–liquid extraction, and the extract was analyzed by gas chromatography with $_{63}Ni$ electron capture detection.

Samples containing alachlor were extracted and analyzed by gas chromatography with electron capture detection according to the procedure described by Badriyha et al. [23]. The chromatograph employed a 6 feet × 4 mm ID glass column packed with 1.5% SP-2250 and 1.95% SP-2401 on 100/120 Supelcoport (Supelco Inc., Bellefonte, PA), and was operated isothermally at 240 °C.

Dissolved sulfide concentrations in aqueous samples at high and low levels were measured by the iodometric and methylene blue methods, respectively [24].

3.2. Methodologies

3.2.1. Membrane filtration experiments

3.2.1.1. Membrane testing apparatus. A crossflow plate-and-frame membrane system was employed for these nanofiltration experiments, as illustrated in Fig. 2. The feed solution was pumped from the feed tank to the stainless steel plate-and-frame membrane cell (SEPA CF membrane cell; Osmonics, Minnetonka, MN), and the flow rate was controlled by adjusting the recirculation flow into the feed tank. The membrane cell contained a flat membrane sheet with an effective membrane area of 155 cm^2. The transmembrane pressure and crossflow velocity were continuously monitored and maintained at desired levels.

3.2.1.2. Operating conditions for nanofiltration tests. The cross-flow rate and the trans-membrane pressure were both maintained at specified values, but that permeate flux was allowed to vary over time. This was so because the permeate flux was controlled by the extent of membrane fouling as a function of time. The membrane element was operated under constant pressure of 120 psig (9 bar), and the cross-flow velocity was maintained at 15 cm/s to simulate the hydrodynamics of a commercial spiral-wound membrane element (i.e., 10–50 cm/s). Both permeate and retentate were recycled back to the feed reservoir to maintain a high feed flow rate of 1.15 L/min. Recycling of retentate and permeate resulted in a gradual decrease in the TOC concentration of feed during filtration due to interactions between the adsorbable NOM fractions and membrane surface. In order to compensate for solute loss, the feed solution was periodically replaced by fresh groundwater. The permeate and crossflow rates were continuously monitored.

3.2.1.3. Membrane cleaning procedures. Three different chemical agents were evaluated: (i) 0.1 M NaOH, (ii) 0.1 M citric acid, and (iii) 0.001 M sodium dodecyl sulfate–SDS [8]. Membranes fouled with raw or preoxidized water were cleaned by filtering one of the chemical agents for 1 h, followed by filtration with DI water for 5–10 min to remove residuals of cleaning agents. Additionally, a cleaning strategy with successive application of caustic and acid solutions was employed, wherein the following sequence was used: caustic cleaning for 20 min, acid cleaning for 20 min, again caustic cleaning for 20 min. Each chemical cleaning step in this sequence was followed by filtration of deionized water for 5–10 min to avoid cross-contamination.

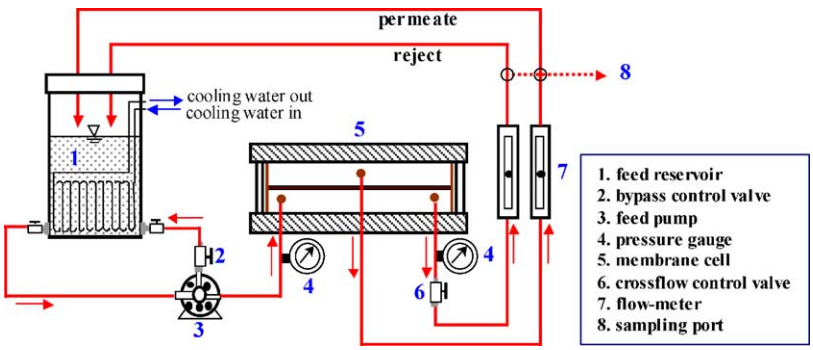

Fig. 2. Schematic diagram of the crossflow membrane filtration unit.

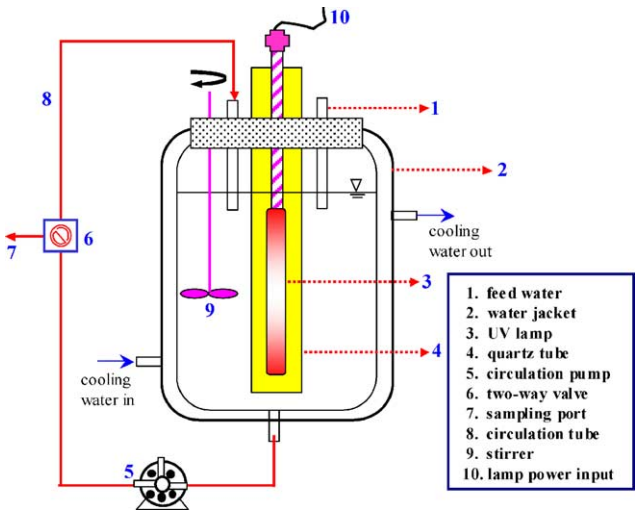

Fig. 3. Experimental setup for H_2O_2/UV pretreatment.

3.2.2. H_2O_2/UV oxidation batch studies

The direct photolysis and H_2O_2/UV oxidation studies were conducted in a 6-L water-jacketed Pyrex reactor (Fig. 3), fitted with a central quartz tube and a UV lamp. The reactor was provided with a stainless steel stirrer, and a recirculation pump with ceramic piston and casing. All circulation tubings were made of either stainless steel or Teflon. The circulation flow rate was maintained at 250 mL/min to achieve conditions of a completely mixed batch reactor, and the reactor temperature was maintained at 25 °C by means of a constant temperature bath. The reactor was filled with 4.5 L of test solution, and the temperature was stabilized prior to the commencement of each experiment. The experimental run was initiated by turning on the UV lamp, and samples were taken before and during these runs for determining the concentrations of TOC, UVA_{254}, UVA_{310}, alachlor, pH, THMFP, hydrogen sulfide, and residual hydrogen peroxide.

3.2.3. Attenuated total reflection-Fourier transform infrared spectroscopy studies

The ATR-FTIR technique was used to investigate functional groups and molecular structures on the membrane surface and deposited foulants. All samples including the virgin, fouled, and cleaned membranes were gently washed with deionized water, and then dried overnight at room temperature. A Perkin-Elmer 2000 FTIR apparatus (Norwalk, CT) equipped with a HeNe [helium compound with neon (1:1)] laser as a radiation source (unpolarized IR radiation), triglycine sulfate as a detector, and optical KBr as a beam splitter was employed. The ATR method was used for recording the IR spectra of the sample, wherein a ZnSe crystal was employed as an accessory. The crystal was operated as an internal reflection element at a nominal angle of incidence of 45°.

3.2.4. X-ray photoelectron spectroscopy studies

The XPS measurements were conducted to determine the chemical composition and nature of elements in the near surface region of the membrane. The samples were placed inside an analytical chamber and allowed to outgas until a pressure less than 1.33×10^{-5} Pa (1×10^{-7} Torr) was attained. The XPS data were obtained using a Perkin-Elmer/Physical Electronics Division Model 5100 X-ray photoelectron spectrometer (Norwalk, CT) with a non-monochromatic Al Kα (1486.6 eV) radiation source operated at 15 kV and 300 W.

3.2.5. Atomic force microscopy studies

The AFM technique was used to image membrane surfaces with a nanometer scale resolution. A commercial AFM liquid cell was used, and the topographic images were obtained from an Autoprobe® CPSPM microscope (Park Scientific Instruments, Sunnyvale, CA). The instrument was operated in a non-contact or tapping (intermittent contact) mode, and the images were obtained by scanning a sharp tip over the membrane surface.

3.2.6. Scanning electron microscopy studies

The SEM technique was also used to further characterize the surface morphology of membrane foulants. The SEM micrographs were obtained using a Cambridge 360 scanning electron microscope (Cambridge Instruments, Woburn, MA), operated at a resolution of 30 Å. The membrane samples were freeze-dried and coated with a thin layer of graphite prior to analysis.

4. Results and discussions

4.1. Effect of H_2O_2/UV pretreatment on permeate flux

The raw water and preoxidized waters under different pretreatment conditions, including UV radiation intensity, hydrogen peroxide dosage, and preoxidation time, were subjected to nanofiltration. Results of nanofiltration tests with raw water and different preoxidized waters are presented in Fig. 4 and Table 3. As can be observed from Fig. 4, preoxidized waters exhibited significantly less permeate flux declines than raw water. Furthermore, between the two preoxidized waters, a longer oxidation time or higher hydrogen peroxide dosage exhibited increase in permeate fluxes. In general, SUVA in the wavelength range 190–350 nm (usually 254 nm) is used to represent hydrophobicity or aromaticity of NOM [11,25]. In this study, SUVA at 310 nm ($SUVA_{310}$) was used specifically for samples containing residual hydrogen peroxide, because the peroxide exhibited absorbance in the 190–300 nm range interfering with UV absorbance measurements at 254 nm [25]. Therefore, a decrease in $SUVA_{310}$ after H_2O_2/UV pretreatment would signify transformation of humic substances into less- or non-humic substances (Table 3). Consequently,

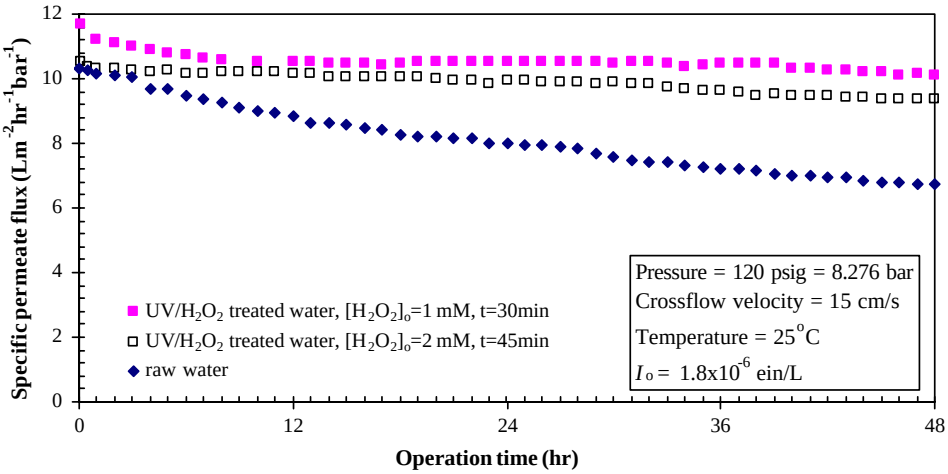

Fig. 4. Permeate flux profiles for nanofiltration performed with raw water and H_2O_2/UV preoxidized waters.

the H_2O_2/UV pretreated water manifested lower membrane fouling potential as compared to the untreated water, and the reasoning behind this observation was based on the following hypotheses. During H_2O_2/UV preoxidation, the reactive functional groups associated with humic substances (that ordinarily demonstrate strong adsorption affinity for the membrane surfaces), were replaced by new functional groups with lower sorption affinities for the membrane surface (Fig. 1). Additionally, major breakdown of NOM macromolecules caused a substantial decrease in hydrophobic interactions with membrane surface, resulting in lower adsorptive organic fouling. Furthermore, lower biological fouling due to destruction of microorganisms could be a reason for the lower fouling tendency of preoxidized waters.

An important consideration in adsorptive membrane fouling could be the charge density of NOM. An increase in organic acid constituents of NOM after preoxidation provides more ligands or sites for calcium complexation, and consequently the negative charge of NOM decreases [26]. Such a decrease in NOM charge may promote adsorptive organic fouling for the negatively charged membranes. Nonetheless, the lower fouling tendency of preoxidized water, based on the permeate fluxes shown in Fig. 4, suggested that decreased hydrophobic interaction due to lower sorption affinity was more influential than a reduction in charge repulsions between the NOM molecules and membrane surface. It must be noted that the hydrogen bonding energies associated with sorption of hydrophobic NOM on membrane surfaces are generally much larger than the electrostatic potential energies associated with charge interactions.

4.2. Effect of H_2O_2/UV pretreatment on the permeate quality

Nanofiltration tests were performed with raw and H_2O_2/UV preoxidized waters to investigate the membrane performance for the removals of NOM, alachlor, and hydrogen sulfide. The findings are presented in the ensuing sections.

4.2.1. NOM removal

4.2.1.1. NOM rejection by nanofiltration alone. The NOM rejection by the nanofiltration membrane was investigated in terms of total organic carbon (TOC), UVA_{254}, color, and 24 h-THMFP. The average rejection for TOC was found to

Table 3
Effect of NOM decomposition on nanofiltration performance

Feed	Permeate flux[a] ($L\,m^{-2}\,h^{-1}\,bar^{-1}$)	TOC (mg/L)[b]		TOC rejection (%)	UVA_{310} (cm^{-1})[b]		$SUVA_{310}$[b] ($mg^{-1}\,L\,cm^{-1}$), feed
		Feed	Permeate		Feed	Permeate	
Raw water	8.11	3.5	0.40	89	0.101	0	0.029
Preoxidized water[c]	9.86	3.3	0.45	86	0.036	0	0.011
Preoxidized water[d]	10.50	2.6	0.50	81	0.017	0	0.007
Preoxidized water[e]	11.45	2.0	0.97	52	0.011	0	0.005

[a] Flux averaged throughout entire filtration time.
[b] Average value for the samples taken every 2 h during 48 h.
[c] UV radiation intensity $= 1.8 \times 10^{-6}$ einstein/L s, $[H_2O_2]_0 = 1$ mM, oxidation time $= 30$ min.
[d] UV radiation intensity $= 1.8 \times 10^{-6}$ einstein/L s, $[H_2O_2]_0 = 2$ mM, oxidation time $= 45$ min.
[e] UV radiation intensity $= 2.4 \times 10^{-6}$ einstein/L s, $[H_2O_2]_0 = 5$ mM, oxidation time $= 45$ min.

be 93%, while those for UVA_{254} and color were comparatively higher at 98 and 99%, respectively, suggesting preferential rejection of the humic or aromatic NOM fractions. The values of 24 h-THMFP in permeate averaged 19 μg/L (93% removal), meeting the proposed maximum contaminant level (PMCL) of 40 μg/L.

4.2.1.2. NOM removal by H_2O_2/UV oxidation alone. A hydrogen peroxide dosage of 2 mM was used under the pretreatment conditions because only marginal improvement in the NOM decomposition efficiency was achieved beyond this level [27]. Although, lowering the solution pH prior to H_2O_2/UV oxidation could increase the NOM decomposition rate [25], it was not considered in the present studies due to expected adverse effects of low pH on permeate flux and NOM rejection, based on previous investigations [1,28]. Under these operating conditions ($[H_2O_2]_0 = 2$ mM and pH 8.3), preoxidation for 30 min significantly reduced UVA_{254}, color, and $SUVA_{254}$ by 42, 41, and 35%, respectively, whereas only marginally reduced the TOC by 9%. The relatively low TOC reductions as compared to UVA_{254} reductions can be explained by the structural changes in NOM composition. For instance, aromatic fractions are transformed into aliphatic fractions, and humic fractions are converted to non-humic fractions, without significant conversion of organic matter to carbon dioxide. Additionally, the average THMFP of 212 μg/L in the preoxidized water suggested that the transformed NOM as well as products generated (such as non-humic substances) still functioned as trihalomethane precursors. Furthermore, it was observed that complete mineralization of NOM did not occur even after exposure to oxidation for a long duration of 30 min, suggesting that greater treatment might be required to meet the current maximum contaminant level (MCL) of 80 μg/L for THMs.

4.2.1.3. NOM removal by nanofiltration with H_2O_2/UV pretreatment. The NOM rejection efficiencies of the nanofiltration membrane with respect to changes in pretreatment conditions are presented in Table 3. As evident, lower TOC rejections were observed for preoxidized waters. The following phenomena could be responsible for lower NOM rejection: (i) decrease in size exclusion due to transformation of macromolecules into lower molecular weight molecules, (ii) reduction in apparent MWCO due to lower NOM deposition on membrane surface, and (iii) decrease in electrostatic exclusion due to the lower negative charges of preoxidized NOM [25]. The average 24 h-THMFP value of the permeate was found to be 25 μg/L, meeting the PMCL criterion. Further, the results (Table 3) depicted that NOM rejection efficiency (measured by TOC) appeared to be inversely proportional to the degree of NOM oxidation (as indicated by $SUVA_{310}$). Lower TOC rejections with increasing hydrogen peroxide dosage, oxidation period, and UV radiation intensity illustrate this aspect. The source water subjected to 30 or 45 min of preoxidation with hydrogen peroxide dosage of 1 or 2 mM and a UV intensity of 1.8×10^{-6} einstein/L, exhibited higher permeate flux (Fig. 4) and slightly lower NOM rejection (Table 3). However, when the feed water was oxidized at higher oxidant dosage and UV intensity ($[H_2O_2]_0 = 5$ mM, $I_0 = 2.4 \times 10^{-6}$ einstein/L, and oxidation time = 45 min), the higher permeate flux was accompanied by a significant increase in the permeate TOC (0.97 mg/L). These results indicated that the operating conditions for preoxidation must be carefully controlled to balance fouling mitigation and NOM rejection. Another influential factor determining the required degree of preoxidation could be the membrane MWCO characteristics. If the H_2O_2/UV preoxidation were followed by relatively higher MWCO membrane as in ultrafiltration, a slight over-oxidation of source water could lead to significant permeate deterioration. This theory was based on the premise that preoxidation would produce smaller organic molecules rejected by low MWCO nanofiltration and reverse osmosis membranes, resulting in greater surface fouling. However, the low MWCO ultrafiltration and microfiltration membranes would facilitate pore transport of organic molecules, eventually causing internal pore fouling and significant flux deterioration.

4.3. Hydrogen sulfide and alachlor removals

The average dissolved sulfide concentration of the raw groundwater was about 570 μg S/L, and nearly 20% of it was reduced during nanofiltration process alone. Such decrease might be caused primarily by evaporation as well as oxidation by atmospheric oxygen during the filtration process, rather than by size or electrostatic rejection. However, H_2O_2/UV oxidation for 30 min with initial hydrogen peroxide concentration of 1 mM and UV radiation intensity of 1.8×10^{-6} einstein/L could achieve a dissolved sulfide removal efficiency of 99.8%, corresponding to a residual dissolved sulfide concentration of 1.2 μg S/L (i.e., 0.24 μg/L as H_2S), well below the threshold odor levels of 100–200 μg/L reported for clean waters.

The raw source water spiked with 100 μg/L of alachlor was subjected to H_2O_2/UV oxidation (i.e., $[H_2O_2]_0 = 1$ mM, $I_0 = 1.8 \times 10^{-6}$ einstein/L) for 30 min, prior to nanofiltration. No alachlor was detected in the pretreated water, and thus no residual was carried over into the nanofiltration process. Although alachlor could be effectively removed by nanofiltration alone, its hydrophobic tendency to be adsorbed onto and subsequently desorbed from the membranes might be a cause for concern.

4.4. Nanofiltration with membrane cleaning

Nanofiltration tests using raw water and H_2O_2/UV pretreated water were performed with periodic membrane cleaning to simulate full-scale plant operations. In order to investigate the long-term effect of chemical cleaning and source water pretreatment on the permeate flux and permeate quality, nanofiltration tests were performed for an extended period of 192 h. These experiments employed

Table 4
Operation setup for nanofiltration with pretreatment and chemical cleaning

Feed	Cleaning agent	Total running time[a]	Cleaning intervals (h)	Figures
Raw water	0.1 M NaOH	192 h (4 cycle)	48	5a, 10d
Preoxidized water	0.1 M NaOH	192 h (2 cycle)	96	5a, 8d
Raw water	0.1 M citric acid	192 h (4 cycle)	48	5b
Preoxidized water	0.1 M citric acid	192 h (2 cycle)	96	5b
Raw water	0.001 M SDS[b]	192 h (4 cycle)	48	5c, 9c
Preoxidized water	0.001 M SDS[b]	192 h (2 cycle)	96	5c
Raw water	Successive cleaning[c]	192 h (4 cycle)	48	6, 7

[a] Excluding the time for membrane cleaning.
[b] Sodium dodecyl sulfate.
[c] Caustic cleaning (20 min), acid cleaning (20 min), and caustic cleaning (20 min) using 0.1 M NaOH and 0.1 M citric acid solutions.

different cleaning intervals of 48 and 96 h for the raw and preoxidized water, respectively, due to their differences in fouling potentials as shown in Table 4. Upon completion of filtration runs (four cycles for raw water and two cycles for preoxidized water), the membranes were chemically cleaned and preserved for surface characterization studies. The effects of the cleaning agent type and pretreatment of source water on permeate flux (and flux recovery) and permeate quality are discussed in the ensuing sections.

4.4.1. Effect of chemical agent type on flux recovery

It is a general theory that flux recovery of a cross-flow module due to membrane cleaning is attributed to a combination of two factors—the dissolution or desorption effect of the cleaning agent, and the hydrodynamic shear stress applied to the foulant layer [7,29]. This theory further assumes that once the fouling layer is disrupted by the applied chemical agent, it is easily removed by hydrodynamic shear.

The permeate flux profiles for nanofiltration tests performed with raw water using three different cleaning agents are presented in Fig. 5a–c. Higher flux recovery was observed for caustic or acid cleaning vis-à-vis surfactant cleaning. Nonetheless, neither of the chemical agents tested in this study completely removed the foulants, and consequently progressive flux deterioration was experienced with increasing filtration cycles. Such long-term flux decline was substantially mitigated by successive caustic and acid cleaning, an approach that proved more effective for flux recovery than caustic or acid cleaning alone, as reflected in Fig. 6. Successive "dual" cleaning by caustic and acidic solutions would remove both acidic and basic fractions of NOM from the membrane, and this technique has been viewed by several researchers as a practical, efficient and cost-effective approach to mitigate membrane fouling and flux decline [7,8,29].

A number of theories can be proposed in support of the results depicted in Figs. 5 and 6. Better flux recovery by caustic cleaning than that by acid cleaning can be attributed to high humic and fulvic acid content (dissolvable in caustic solution) and low inorganic content (low deposition potential) of the groundwater used (Table 1). Under the high pH conditions experienced in caustic cleaning, the NOM molecules attain more conformational linearity [30,1], and consequently the foulant layer becomes looser and sparser, so that the membrane is better amenable to cleaning. Furthermore, it is hypothesized that the hydroxyl ions in caustic solution (0.1 M NaOH) could promote disruption of the fouling layer by these mechanisms: (i) increasing ionic strength, (ii) increasing solubility of NOM foulants, and (iii) decreasing negative charge of NOM and membrane due to adsorption of sodium ions [29].

In order to measure gradual flux increase during successive chemical cleaning with caustic and acid solutions, deionized water was applied to the membrane for a short duration (5–10 min) immediately after each cleaning (20 min) and the flux was measured. The initial specific flux depicted in Fig. 7 was $13\,m^{-2}\,h^{-1}\,bar^{-1}$. It can be observed from Fig. 7 that most flux recovery (over 97%) was witnessed after the first caustic cleaning cycle. Further increase in the flux after acid cleaning might suggest that some residual foulants after caustic cleaning, such as calcium-bound organic acid constituents, were removed by acid cleaning. Similar effects were observed by Hong and Elimelech [30], when a membrane fouled with calcium-complexed NOM was cleaned successively with caustic (pH 10) and EDTA (10^{-3} M) solutions. These investigators suggested that EDTA could remove calcium from NOM foulants through a ligand-exchange reaction resulting in more negative charge of NOM (increased electrostatic repulsion among the NOM foulants). Similarly, they proposed a ligand-exchange reaction between NOM–calcium complexes and citric acid during acid cleaning. Nonetheless, it must be noted that acid cleaning might not remove unbound organic acid constituents (which used to be complexed with calcium) because these organic acids are protonated and coiled with other organic foulants under acidic conditions (pH < 2) [28,30].

It was suggested that during the deionized water rinsing after acid cleaning (pH ~ 5), some of stronger carboxylic groups (amenable to deprotonation in the pH range 3–6) were removed; however, weak carboxylic acid constituents (that could be deprotonated only in the pH range 6–10) was not removed [25]. These weak carboxylic acid constituents

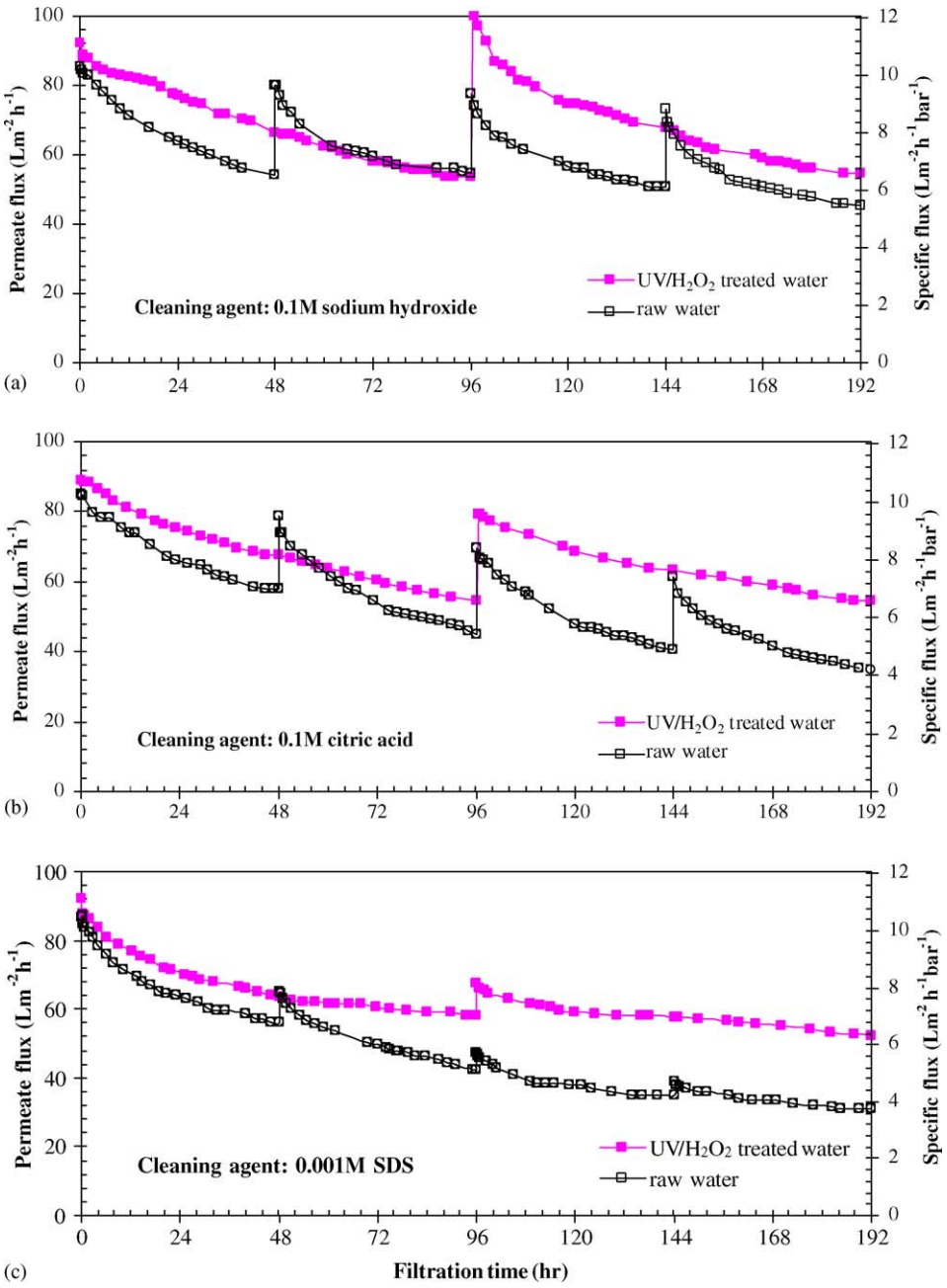

Fig. 5. Effect of the H_2O_2/UV pretreatment on permeate flux for various membrane cleaning strategies: (a) caustic cleaning, (b) acid cleaning, and (c) surfactant cleaning.

were apparently removed by the second caustic cleaning, a hypothesis supported by the flux increase shown in Fig. 7. Nonetheless, it must be noted that the flux progressively decreased with increasing number of filtration cycles immediately after the successive cleaning, suggesting the gradual accumulation of residual foulants. A high possibility existed that hydrophobic bases and neutral species adsorbed onto the virgin polyamide membranes could not be desorbed in either acid or caustic solutions due to their hydrophobic interactions with membrane surfaces [28,31]. It is perhaps likely that to the extent that such components were adsorbed onto previously deposited foulant, they would be removed if the original foulant layer were disrupted by hydrodynamic shear.

4.4.2. Effect of preoxidation on flux recovery

The impact of H_2O_2/UV pretreatment on permeate flux decline and recovery using different cleaning agents is illustrated in Fig. 5a–c. In general, higher permeate fluxes were observed for preoxidized water than for raw water, despite the lower cleaning frequencies. This is an important factor because a lower cleaning frequency might significantly enhance the membrane life and performance. Pre-

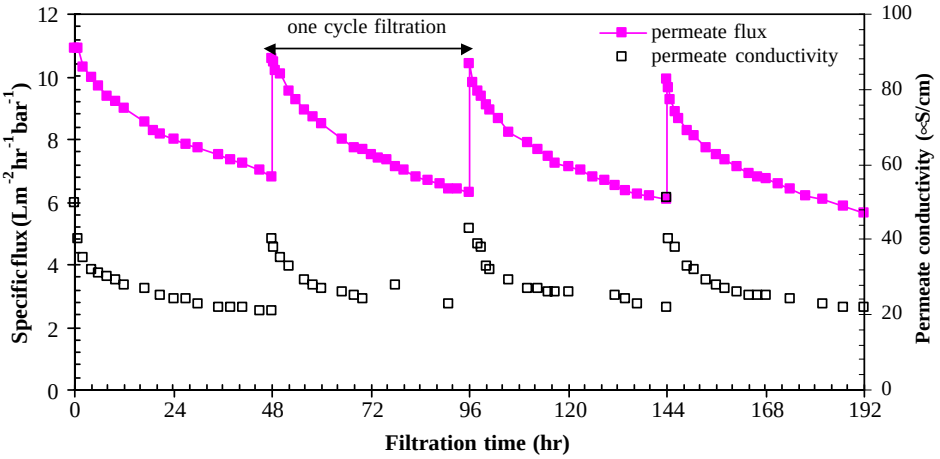

Fig. 6. Permeate flux profiles and permeate conductivity for nanofiltration tests performed with raw water using successive cleaning with caustic and acid solutions.

oxidation was found to improve the caustic cleanability of membrane, as indicated by the flux recovery results presented in Fig. 5a, attributable to the lower sorption affinity of preoxidized NOM constituents for the membrane surface. Furthermore, preoxidation increased the organic acid constituents of NOM [25], a factor that might have contributed to better flux recovery during caustic cleaning. In the case of preoxidized water, the permeate flux immediately after caustic cleaning was even higher than the initial flux, possibly due to the removal of preservative (sodium azide applied by the manufacturer). The fouling mitigation achieved by preoxidation appeared similar to that accomplished by acid or surfactant cleaning, manifesting an overall higher permeate flux for preoxidized water with lower cleaning frequency (Fig. 5b and c). However, with acid or surfactant cleaning there were no marked differences in flux recoveries, an observation which suggested that preoxidation had no significant effect on the efficiency of acid or surfactant cleaning.

4.4.3. *Effect of preoxidation and chemical cleaning on permeate quality*

Table 5 lists the average values of the feed and permeate quality parameters. Similar values for color, UVA_{254}, and conductivity of permeate waters were observed regardless of the cleaning agent and feed pretreatment employed. However, somewhat different average permeate TOC concentrations were observed for different cleaning agents. For example, relatively low values of permeate TOC were obtained with anionic surfactant as compared to other cleaning agents. This can be hypothetically explained by the following mechanisms: (i) more negative charge density of the membrane surface due to the adsorption of the surfactant molecules having negatively charged sulfate functional groups, namely, increased electrostatic exclusion, and (ii) decrease in apparent MWCO due to ineffective foulant removal by surfactant cleaning.

The average permeate TOC concentrations with acid cleaning were shown to be higher than those with other

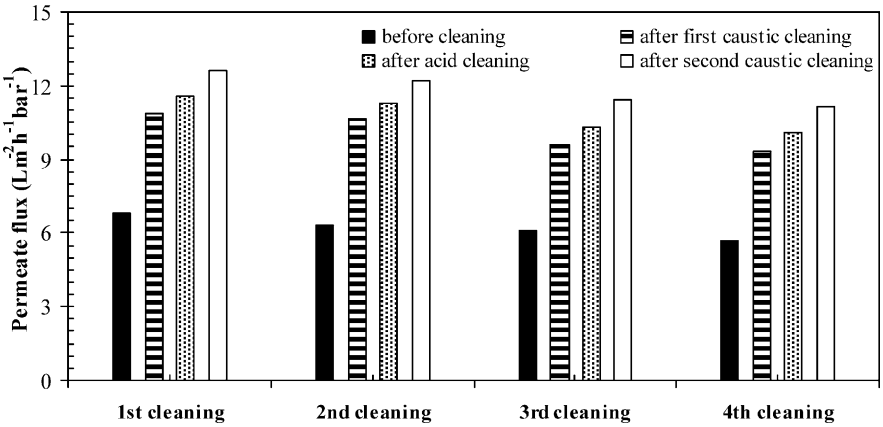

Fig. 7. Permeate flux recovery during the successive cleanings with caustic and acid solutions for the NOM-fouled membrane (as measured by DI water flux immediately after each chemical cleaning).

Table 5
Permeate qualities[a] with different membrane cleaning strategies

Cleaning strategy	Feed	TOC (mg/L)		Conductivity (μS/cm)		Color (Pt–Co)		UVA_{254} (cm^{-1})	
		Feed	Permeate	Feed	Permeate	Feed	Permeate	Feed	Permeate
Caustic cleaning	Raw water	3.54 ± 0.07	0.49 ± 0.04	368 ± 3	28 ± 3	73.4 ± 3.1	0.1	0.181 ± 0.003	0.000
	H_2O_2/UV treated water	3.25 ± 0.07	0.55 ± 0.05	365 ± 2	28 ± 3	22.3 ± 3.4	0.3	0.059 ± 0.007	0.008[b]
Acid cleaning	Raw water	3.56 ± 0.12	0.81 ± 0.28	363 ± 2	24 ± 2	77.6 ± 2.5	0.7	0.186 ± 0.007	0.001
	H_2O_2/UV treated water	3.30 ± 0.08	0.59 ± 0.13	355 ± 2	26 ± 3	21.7 ± 5.2	0.6	0.061 ± 0.009	0.008[b]
Surfactant cleaning	Raw water	3.47 ± 0.07	0.42 ± 0.05	360 ± 2	27 ± 2	80.6 ± 2.5	0.5	0.187 ± 0.003	0.001
	H_2O_2/UV treated water	3.24 ± 0.06	0.46 ± 0.07	363 ± 1	26 ± 2	14.8 ± 2	0.4	0.059 ± 0.007	0.009[b]
Successive cleaning	Raw water	3.48 ± 0.07	0.50 ± 0.04	356 ± 2	29 ± 2	72.6 ± 3.6	0.2	0.189 ± 0.004	0.000

[a] Average value with 95% confidence interval for the samples taken every 4–8 h during 192 h.
[b] UVA_{254} primarily caused by residual hydrogen peroxide present in the sample.

chemical agents. A plausible explanation for the drastic increase in permeate TOC immediately after acid cleaning could be that unlike after caustic cleaning, foulant removal and flux recovery were mainly accomplished in the case of deionized water and groundwater, and this could be due to the increased electrostatic repulsion among NOM foulants at neutral pH. This was evident from the deep brown color of the permeate and retentate. Such foulant releases were shown to proceed over extended periods of several hours, as indicated by the high permeate TOC levels. The high TOC levels (2.7–4.3 mg/L) and extremely low UVA_{254} values ($<0.003\,cm^{-1}$) for the permeate seemed to indicate that among the released foulants low molecular-weight aliphatic molecules were not well rejected by the nanofiltration membrane, as observed by previous researchers [28,31,18].

High TDS rejection efficiencies were observed both for raw and preoxidized water filtrations based on conductivity data. The TDS rejection rates appeared quite stable regardless of cleaning agent used, although the rejections exhibited somewhat different trends before and after membrane cleaning. At the beginning of filtration or immediately after membrane cleaning, the permeate conductivity values were about 40 μS/cm; however, as more NOM deposited on the membrane surface, the value decreased to about 20 μS/cm (Fig. 6).

4.5. Membrane surface characterization studies

Nanofiltration membranes at various stages of filtration operation were characterized by surface analysis, a summary of which is provided in Table 6. Membrane samples were divided into the following categories: (i) virgin membrane to serve as a control, (ii) membrane used for filtering raw water and preoxidized water for 48 h, (iii) membrane exposed to one cycle of filtration with subsequent cleaning, and (iv) membrane exposed to several cycles of filtration with periodic cleaning.

Table 6
Elemental composition of membrane surfaces as determined by XPS

Membrane samples					Atomic composition[b] (%)			
Sample no.	Status	Cleaning agent	Feed	Time (h)	C	O	N	Ca
1	Virgin	–	–	–	63.7	22.7	11.9	0.0
2	Virgin[a]	–	–	–	64.0	19.4	12.3	0.0
3	Fouled	–	Raw	48	69.1	24.1	3.7	0.8
4	Fouled	–	Preoxidized	48	60.4	25.9	4.5	0.3
5	Cleaned	Caustic	Raw	48	63.0	28.3	6.7	0.3
6	Cleaned	Caustic	Preoxidized	48	64.5	25.4	8.4	0.5
7	Cleaned	Caustic	Raw	192	66.1	25.5	3.7	0.4
8	Cleaned	Caustic	Preoxidized	192	63.9	25.8	7.6	0.4
9	Cleaned	Acid	Raw	192	64.6	28.4	6.1	0.0
10	Cleaned	Acid	Preoxidized	192	NA[c]	NA	NA	NA
11	Cleaned	Surfactant	Raw	192	70.7	22.3	5.3	0.2
12	Cleaned	Surfactant	Preoxidized	192	68.1	25.5	2.6	<0.1

[a] Virgin membrane soaked in H_2O_2 solution.
[b] Na, Z, Cu, Fe, and Cl are found at trace levels.
[c] Not analyzed.

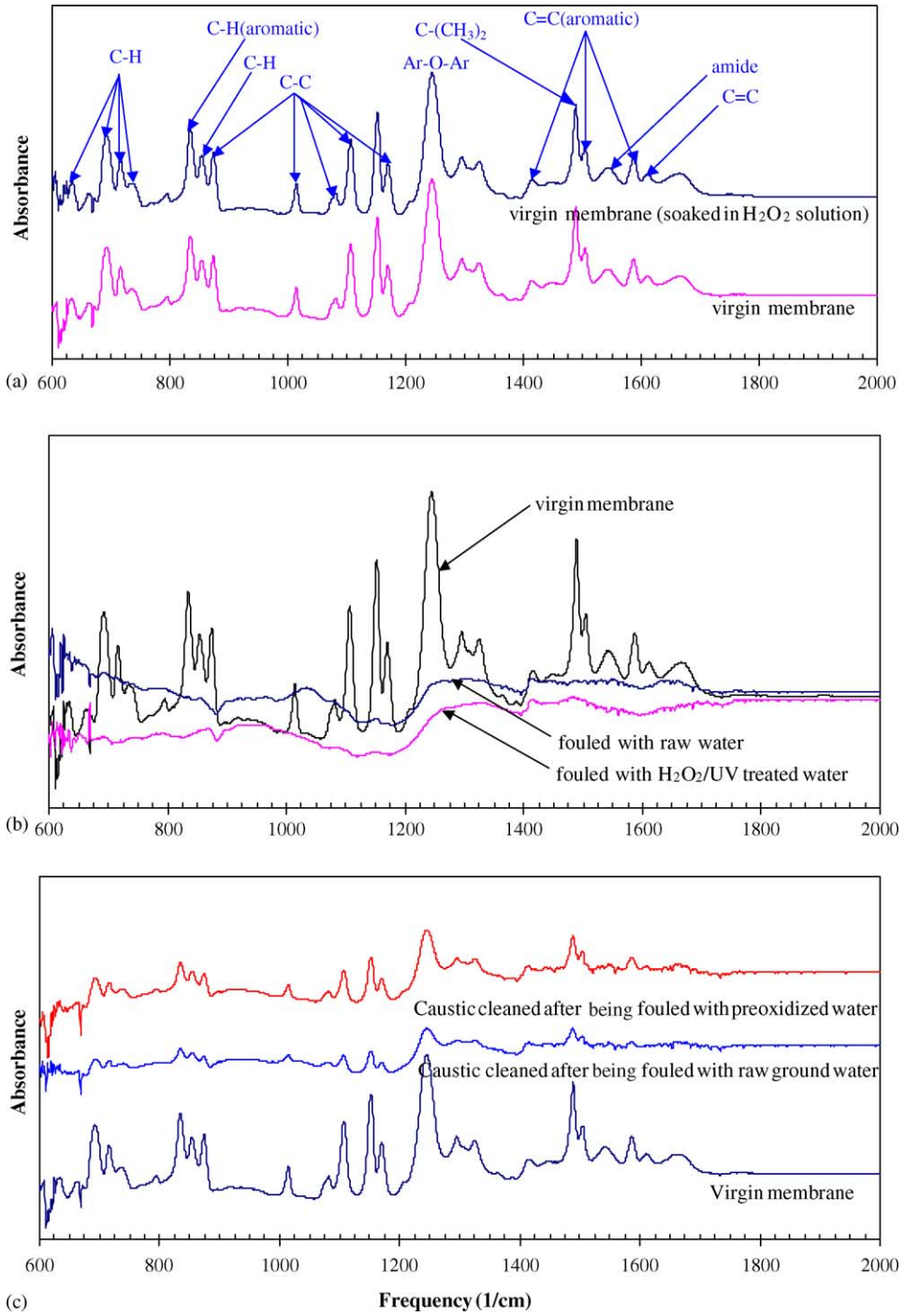

Fig. 8. The FTIR spectra of membranes at various phases of membrane operation: (a) virgin membranes, (b) fouled membranes, and (c) caustic-cleaned membranes.

4.5.1. Attenuated total reflection-Fourier transform infrared spectroscopy studies

The FTIR spectrum for a typical virgin NF70 membrane, presented in Fig. 8a, reflects the typical pattern expected of polyamide or polysulfone membranes [16,7]. The principal absorption bands for the virgin membrane consist of frequencies or wave numbers associated with these bond characteristics: ν_{CH} (C–H rocking) vibrations at 635–855 cm^{-1}, ν_{CC} (C–C stretching) stretching at 875–1110 cm^{-1}, ν_{COC} (aromatic ring–O–aromatic ring) stretching vibrations at 1240 cm^{-1}, and ν_{CC} (C=C stretching in the aromatic rings) vibrations at 1410, 1500, and 1580 cm^{-1}. The FTIR spectrum of the virgin membrane soaked in hydrogen peroxide (5 mM) for 1 month is also presented in Fig. 8a. The two spectra were identical (Fig. 8a) highlighting the fact that the virgin membrane did not undergo any change in structure

or composition on exposure to hydrogen peroxide because the oxidant reacts only with water-soluble polymers.

The FTIR spectra for the fouled membranes are shown in Fig. 8b. It can be seen that the absorption peaks in the virgin membrane spectra were either eliminated or severely attenuated due to coating by NOM foulants. However, the spectral bands between wave numbers 950 and 1200 cm^{-1} were significantly stronger in intensity for the membrane fouled with raw water, as compared to the virgin membrane. These peaks apparently originated from the polysaccharides in NOM foulants, as possible assignments can be made to the C–O–C vibrations of polysaccharides at frequencies of 1050 and 1080 cm^{-1} [32]. In contrast, these peaks were not observed for the membrane fouled with preoxidized water (Fig. 8b), indicating that organics with high fouling potential (polysaccharides) were transformed into those with relatively low fouling potential during H_2O_2/UV oxidation. Furthermore, as the spectral bands for membrane exposed to preoxidized water were weaker in intensity than that for membrane exposed to raw water, it appears that NOM constituents in raw water were transformed into less adsorbable substances during preoxidation. The mechanistic hypothesis presented here are well supported by the permeate flux profiles for raw and preoxidized waters (Figs. 4 and 5).

The FTIR spectra for caustic-cleaned membranes after 48 h of filtration are presented in Fig. 8c. The absorption bands for caustic-cleaned membrane after being fouled with either raw or preoxidized water were significantly decreased in intensity, as compared to those for the virgin membrane at the following frequency or wavenumber ranges: vibrations at 635–855 cm^{-1} (C–H rocking), stretching at 875–1110 cm^{-1} (C–C stretching), stretching vibrations at 1240 cm^{-1} ν_{COC} (C–O–C stretching between two aromatic rings), and vibrations at 1410, 1500, and 1580 cm^{-1} (C=C stretching in aromatic rings). Nevertheless, a comparison of the spectra for the two caustic-cleaned membranes, one exposed to raw water and the other exposed to preoxidized water, indicated that the latter had better peak recovery after cleaning. These observations supported the theory, based on flux recovery data, that foulants from preoxidized water were cleaned more effectively than those from raw water (Fig. 5a). Furthermore, the observations indicated that preoxidation enhanced caustic cleanability of membranes because the foulants were predominantly smaller organic acids removable by reactions with alkaline solutions.

4.5.2. X-ray photoelectron spectroscopy studies

A survey scan of the skin layer of the virgin membrane primarily detected carbon, oxygen, and nitrogen. The atomic concentrations of these three components agreed well with those from a typical polyamide structure reported by previous investigators [33,13], as shown in Table 6. Additionally, sodium, zinc, copper, iron, chlorine, and silicon were detected at trace levels. The relative amounts of calcium present in the fouled and cleaned membranes are presented in Table 7. Although calcium was not detected on the virgin membrane, the metal was found on fouled and caustic-cleaned membranes, as indicated by the Ca($2p_{3/2}$) binding energies of 347.2–347.8 eV. These observations were similar to those of Jucker and Clark [17], and Schäfer et al. [13], who identified organically bound calcium in their samples at binding energies of 349.8 and 349.6 eV, respectively.

After acid cleaning no residual calcium was found due to the release of intramolecular calcium and dissolution of inorganic deposits at low pH (Table 7). Caustic cleaning showed the largest calcium content on membranes as compared to acid or anionic surfactant cleaning. Similar results were reported by Lindau and Jönsson [6], who noted that the iron content of organic foulants increased significantly after caustic cleaning. These observations could be theoretically explained by the following hypothesis. The extent of complexation between organic acid constituents and calcium (or iron) increases during caustic cleaning due to increased availability (deprotonation) of carboxylic acids and oxalic acid of NOM at high pH values [6,29]. The

Table 7
Relative amount of calcium on membranes as determined by XPS

Sample no.[a]	Membrane samples	Calcium (at.%)	Ca($2p_{3/2}$) B.E. (eV)[b]
1	Virgin membrane	0.0	No peak
2	Virgin membrane soaked in hydrogen peroxide (H_2O_2) solution	0.0	No peak
3	Fouled with raw water (1 cycle)	0.8	347.5
4	Fouled with preoxidized water (48 h)	0.3	347.2
5	Caustic-cleaned after fouling with raw water (1 cycle)	0.3	347.6
6	Caustic-cleaned after fouling with preoxidized water (1 cycle)	0.5	347.4
7	Caustic-cleaned membrane (4 cycles)	0.4	347.5
8	Caustic-cleaned after fouling with preoxidized water (1 cycle)	0.4	347.2
9	Acid-cleaned membrane (4 cycles)	0.0	no peak
10	Acid-cleaned after fouling with preoxidized water (1 cycle)	NA[c]	NA[c]
11	Surfactant cleaned membrane (4 cycles)	0.2	347.8
12	Surfactant-cleaned after fouling with preoxidized water (1 cycle)	<0.1	347.6

[a] Number of membrane samples listed in Table 6.
[b] Binding energy in electron volt.
[c] Not analyzed.

calcium-complexed NOM constituents adsorbed onto the negatively charged membrane surface are not desorbed during caustic cleaning due to their low charge density vis-à-vis other deprotonated acids. Thus, gradual accumulation of these residual foulants after repeated caustic cleaning could cause progressive deterioration in permeate flux, a factor that could be more pronounced for feed waters containing moderate or high levels of calcium (the calcium level in the source water was below 10 mg/L). In such situations, successive cleaning with caustic and acid solutions would constitute an effective strategy for permeate flux recovery.

As previously noted, H_2O_2/UV preoxidation could lead to less negative charges on NOM molecules [12,14]. It is hypothesized that association of NOM with calcium would reduce the NOM charge density, and thereby promote sorption of NOM on negatively charged membranes. However, the calcium content of foulants from preoxidized water is lower than that from raw water (0.3% versus 0.8%), as presented in Table 7. A possible explanation is that upon preoxidation calcium-complexed NOM constituents were not necessarily adsorbed on the membrane surface due to lower sorption affinities of preoxidized NOM. This further supports the theory that hydrophobic interactions between NOM and membrane surfaces were more influential than electrostatic interactions. The superior flux recovery by caustic cleaning, as evidenced in Fig. 5a, supports the hypothesis that a lower calcium content of the foulants is a very important factor in promoting the observed improvement in "cleanability" under preoxidized conditions.

The negative charge on the membrane surface mainly originates from the dissociation of acidic functionalities such as carboxylic groups. Therefore, the relative amounts of carbonyl-carbon containing functional groups such as the carboxylic groups shown in Table 8 can be considered to be a surrogate indicator for charge density on the membrane surface. This table provides the relative concentrations of various "carbon containing" functional groups obtained from high-resolution scans of the C(1s) region using XPS. The virgin membrane (sample 1) exhibited larger composition of C(1s) peak at binding energies of 288.2–288.8 eV (peak 3) than the fouled membrane (sample 3), that is, 16 and 9% for virgin and fouled membranes, respectively. These results suggested that carboxylic groups on the virgin membrane surface were coated with NOM foulants that contained a smaller amount of acidic functional groups (than the membrane surface), resulting in an overall surface charge reduction. As a fouled membrane was cleaned using caustic solution (sample 7), the relative amount of C(1s) signal in peak 3 increased from 9 (sample 3) to 11% (sample 7). The caustic-cleaned membrane used in the filtration of preoxidized water (sample 6) exhibited slightly higher carbonyl-carbon content (12%), as compared to the cleaned membrane exposed to raw water (11% for sample 5). However, this carbonyl-carbon content was still lower than those observed for virgin membranes (12% versus 16%), demonstrating that caustic cleaning could not completely remove foulants from preoxidized water. It was also observed that there was no increase in the C(1s) peak 3 size (9%) after surfactant cleaning (samples 3 and 11), consistent with the fact that there was no permeate flux recovery (Fig. 5c).

4.5.3. Atomic force microscopy studies

The AFM images for virgin and fouled membranes are presented in Fig. 9a–c. A significant difference is observed between the surface morphologies of the virgin and fouled membranes, reflected by their root mean square (rms) surface roughness values. The virgin membrane exhibits an rms surface roughness of 48 nm (Fig. 9a), significantly lower than the values for fouled membranes. Fig. 9b shows an AFM image for the membrane exposed to preoxidized water without cleaning (sample 4 in Table 6). This membrane can be regarded as moderately fouled based on the permeate flux of 9.3 L m^{-2} h^{-1} bar^{-1} (Fig. 4), and it has a high surface roughness of 124 nm. The increase in surface roughness can be explained by the following theory. During the initial stages of filtration, macromolecules such as humic or hydrophobic NOM fraction as well as less negatively charged NOM constituents (such as calcium-bound NOM) preferentially deposit onto the negatively charged membrane surface [34].

The surface morphology of the membrane subjected to four cycles of filtration with surfactant cleaning is shown in Fig. 9c. This membrane can be regarded as severely fouled (after 192 h) because of the ineffective foulant removal by surfactant cleaning (Fig. 5c). Further deposition of NOM (192 h) resulted in a decrease in rms surface roughness to

Table 8
Relative composition of total C(1s) peak as determined by XPS

Sample no.[a]	Membrane	C(1s) peak #1 (C–C, C–H)		C(1s) peak #2 (C–NH)		C(1s) peak #3 (C=O)	
		%	B.E (eV)	%	B.E (eV)	%	B.E (eV)
1	Virgin	66	285.0	18	286.5	16	288.2
3	Fouled	72	285.0	19	286.8	9	288.7
4	Less fouled	66	285.0	23	286.7	11	288.6
6	Well-cleaned	70	285.0	18	286.9	12	288.5
5	Moderately cleaned	67	285.0	22	286.7	11	288.5
11	Severely fouled	67	285.0	24	286.9	9	288.8

[a] Number of membrane samples listed in Table 6.

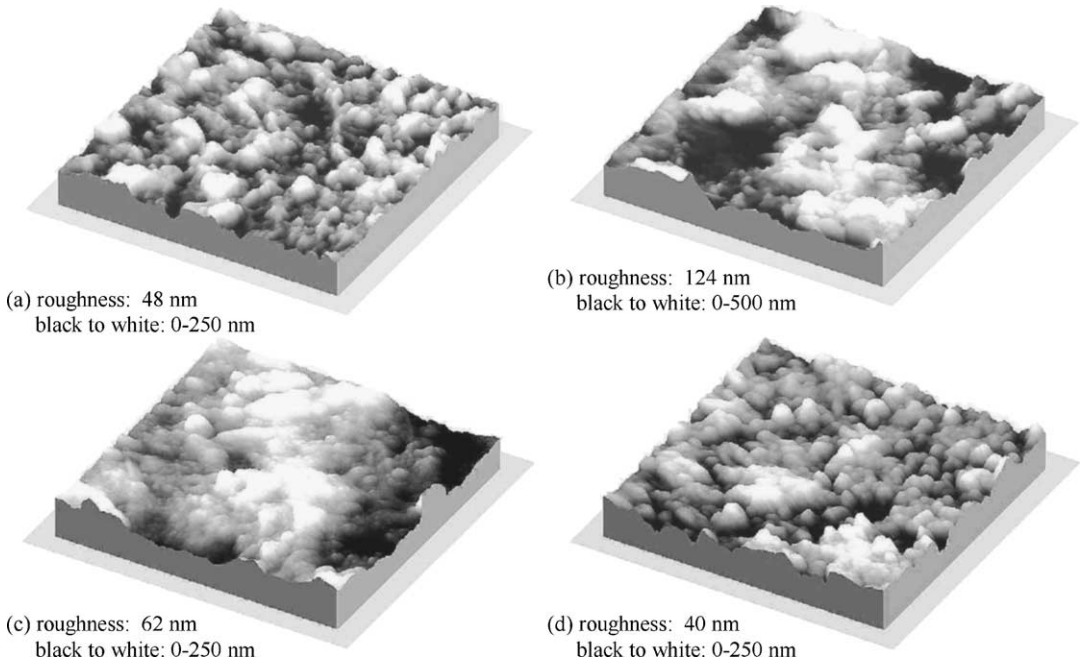

Fig. 9. AFM image scans: (a) virgin membrane (sample 1), (b) fouled with preoxidized water (sample 4), (c) surfactant-cleaned (sample 11), and (d) caustic-cleaned (sample 8).

72 nm, probably due to NOM adsorption onto the depressions in the accumulated foulant layer. According to the conceptual model of NOM adsorption onto membrane surface proposed by Lahoussine-Turcaud et al. [34], this stage of NOM adsorption, referred to as stage II by the investigators, can be regarded as solute accumulation in a densely compacted layer. The caustic-cleaned membrane after two cycles of filtration with preoxidized water (Fig. 9d) exhibited a morphology similar to that of virgin membrane, but had a lower surface roughness (40 nm versus 48 nm). This decreased roughness was presumably caused by residual foulants (such as calcium-bound organic acid constituents) within the concavity of the membrane surface even after caustic cleaning. It can be hypothesized that incomplete removal of organic foulants during caustic cleaning was due to one or the combination of these factors: (a) calcium-complexed NOM constituents with low charge density are formed that might promote fouling; (b) membrane surface roughness could lead to some irreversible deposition of foulants; and (c) hydrophobic interactions between non-desorbable NOM components and membrane surface could cause irreversible fouling.

4.5.4. Scanning electron microscopy studies

The SEM results presented in Fig. 10a–d are based on multiple samples of fouled membranes of the same types to avoid problems associated with cell losses arising from random sample choice (cut pieces of the membranes) and/or sample preparation. The SEM slides presented are therefore typical representatives of those obtained during the multiple analyses. The SEM micrograph of the virgin membrane (Fig. 10a) exhibited the "ridge and valley network" microstructure typical of a polyamide barrier layer [33], while the micrographs of the fouled membranes (Fig. 10a and c) exhibited different surface morphologies. These observations supported the fact that surface adsorption was the main fouling mechanism in nanofiltration membranes [31]. The SEM micrograph of a membrane moderately fouled with preoxidized water after 48 h of filtration (Fig. 10b) showed a somewhat sparse and loosely woven foulant layer due to regional adsorption of macromolecules and the uneven nature of NOM deposition. This type of NOM adsorption might be regarded as stage I of the "staged adsorption model" suggested by Lahoussine-Turcaud et al. [34], according to which dissolved macromolecules were loosely bound to the membrane surface. The uneven structure of foulant deposition was consistent with the large surface roughness reflected by the AFM images (Fig. 10b), and the loose and sparse structure certainly eased chemical cleaning and/or hydraulic rinsing.

The membrane fouled with raw water after 48 h of filtration (Fig. 10c) exhibited a relatively smooth surface. This was consistent with the decreased surface roughness of the severely fouled membrane due to NOM adsorption onto depression areas of the accumulated foulant layer (Fig. 10c). It could be theorized that once a densely compacted gel layer was formed, further accumulation of NOM did not significantly influence the surface morphology (possibly due to hydrodynamic shear of crossflow), but merely increased the layer thickness up to a steady-state value reached between adsorption and desorption [31]. In this regard, the term "morphology" mainly referred to "surface roughness" and "microbial deposition." In our study, fouled membranes after four cycles exhibited visually thicker foulant layers as compared to those only after one cycle, suggestive of such

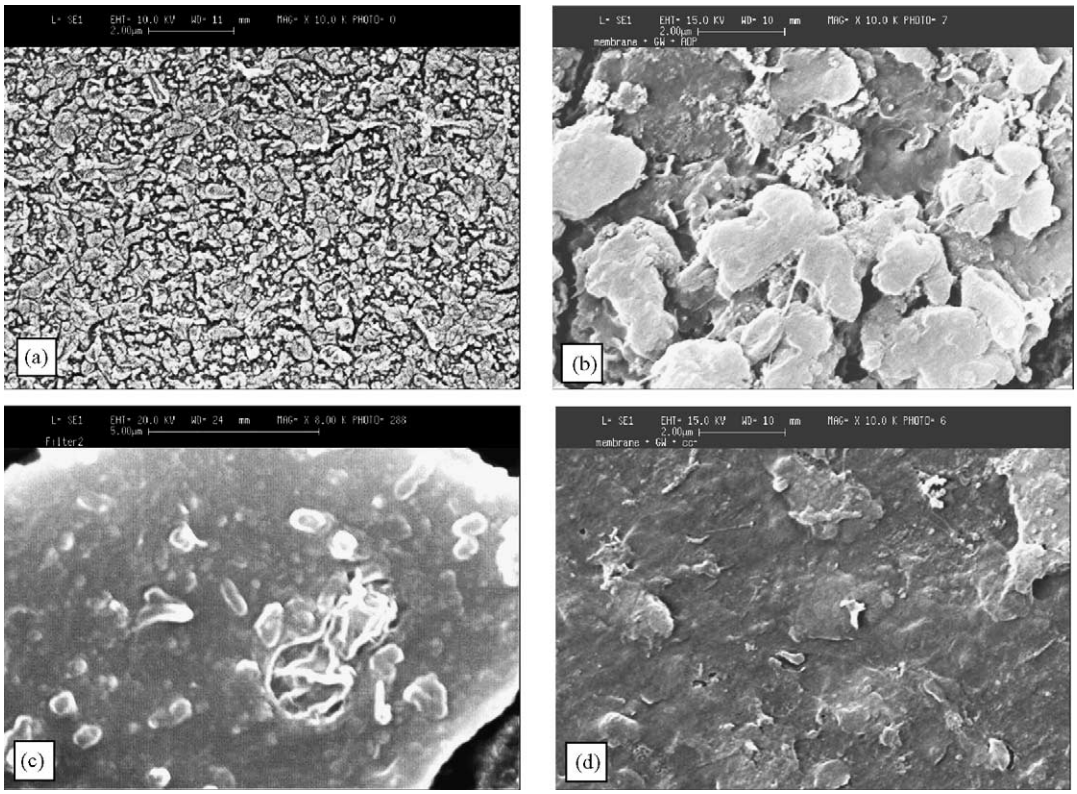

Fig. 10. Scanning electron micrographs: (a) virgin membrane (sample 1), (b) fouled with preoxidized water (sample 4), (c) fouled with raw water (sample 3), and (d) caustic-cleaned (sample 7).

progressive adsorption phenomena. Additionally, Fig. 10c also showed the occurrences of rod-shaped microorganisms on the foulant surface; however, these microorganisms were not observed on membranes exposed to preoxidized water (Fig. 10b). Speth et al. [3] attributed high concentrations of polysaccharides and amino sugars in foulants to the likely presence of bacterial cells (amino sugars) and extracellular materials (polysaccharides). It appeared from the above observations that a strong bonding was necessary to overcome charge repulsion and establish the binding between bacterial cells and NOM foulants. These results were supported by the FTIR spectra for the membrane fouled with raw water which exhibited peak intensities at 1050 and 1080 cm^{-1}, frequencies (wave-numbers) diagnostic for presence of polysaccharides (Fig. 8b).

The membrane subjected to four cycles of filtration with caustic cleaning after each cycle (Fig. 10d) showed a morphology similar to those of foulants from raw water (Fig. 10c), but without the entrapment of bacterial cell fragments, confirming the effectiveness of caustic cleaning in removing biological foulants. Nonetheless, the smooth surface shown in Fig. 10d demonstrated that concavities in the virgin membrane were completely masked by residual foulants after caustic cleaning, an observation consistent with the gradual flux deterioration observed on increasing filtration cycles (flux profile for raw water, Fig. 5a). It should be noted that unlike the caustic-cleaned membrane after exposure to raw water (Fig. 10d), the caustic-cleaned membrane after exposure to preoxidized water exhibited nearly the same surface morphology as the virgin membrane (Fig. 9d). This observation suggested that the preoxidized water might have contained fewer NOM fractions that were non-desorbable.

5. Summary and conclusions

The major findings of this study are briefly summarized as follows:

- The H_2O_2/UV oxidation pretreatment of source water significantly mitigated organic fouling by transforming humic/hydrophobic NOM fractions and polysaccharides into less sorbable organic acids, as investigated by FTIR, XPS, SEM, and AFM. It also provided an effective means for removing hydrogen sulfide and the pesticide alachlor.
- The H_2O_2/UV pretreatment also exhibited the potential to mitigate biological fouling based on the findings from SEM studies further supported by FTIR spectral peaks arising from polysaccharides (extracellular materials) observed only for foulants from raw water.
- The membranes fouled with H_2O_2/UV-pretreated water appeared more amenable to caustic cleaning than those fouled with raw water. This was presumably due to the

lower sorption affinity of preoxidized NOM, increased amount of organic acid constituents, and transformation of non-desorbable NOM fractions into readily desorbable organic substances. This hypothesis was supported by results from ATR-FTIR, XPS, AFM, and SEM studies.

- The chemical cleaning agents tested could not achieve complete flux recovery because residual foulants were strongly embedded in the concavities of membrane surfaces, as reflected by AFM studies. It was found that caustic cleaning could be more effective for permeate flux recovery if preoxidation were employed.

Acknowledgements

This study was partially supported by an NSF, NSE, DMI-0209678 grant. We would like to extend our appreciation to Michael Quinlan, Alan Kershaw, and Roland Resch, for their diligent assistance in various aspects of this research.

References

[1] K.L. Jones, C.R. O'Melia, Protein and humic acid adsorption onto hydrophilic membrane surfaces: effects of pH and ionic strength, J. Membr. Sci. 165 (1) (2000) 31–46.
[2] C.F. Lin, T.Y. Lin, O.J. Hao, Effects of humic substance characteristics on UF performance, Water Res. 34 (4) (2000) 1097–1106.
[3] T.F. Speth, A.M. Gusses, R.S. Summers, Evaluation of nanofiltration pretreatments for flux loss control, Desalination 130 (1) (2000) 31–44.
[4] M. Pirbazari, B.N. Badriyha, V. Ravindran, MF-PAC for treating waters contaminated with natural and synthetic organics, J. Am. Water Works Assoc. 84 (12) (1992) 95–103.
[5] G. Crozes, C. Anselme, J. Mallevialle, Effect of adsorption of organic matter on fouling of ultrafiltration membranes, J. Membr. Sci. 84 (1–2) (1993) 61–77.
[6] J. Lindau, A.S. Jönsson, Cleaning of ultrafiltration membranes after treatment of oily waste-water, J. Membr. Sci. 87 (1–2) (1994) 71–78.
[7] H. Zhu, M. Nyström, Cleaning results characterized by flux, streaming potential and FTIR measurements, Colloids Surf. A Physicochem. Eng. Aspects 138 (2–3) (1998) 309–321.
[8] H. Lee, G. Amy, J.W. Cho, Y.M. Yoon, S.H. Moon, I.S. Kim, Cleaning strategies for flux recovery of an ultrafiltration membrane fouled by natural organic matter, Water Res. 35 (14) (2001) 3301–3308.
[9] S.C. Tu, V. Ravindran, W. Den, M. Pirbazari, Predictive membrane transport model for nanofiltration processes in water treatment, AIChE J. 47 (6) (2001) 1346–1362.
[10] S.W. Benson, Thermochemical Kinetics, 2nd ed., Wiley, New York, 1976.
[11] J. Hoigné, B.C. Faust, W.R. Haag, F.E. Scully, R.G. Zepp, Aquatic humic substances as sources and sinks of photochemically produced transient reactants, in: I.H. Suffet, P. MacCarthy (Eds.), Aquatic Humic Substances: Influence on Fate and Treatment of Pollutants, Advances in Chemistry Series, vol. 219, American Chemical Society, Washington, DC, 1989, Chapter 23, pp. 363–381.
[12] O. Backlund, Degradation of aquatic humic material by ultraviolet light, Chemosphere 25 (12) (1992) 1869–1878.
[13] A.I. Schäfer, A.G. Fane, T.D. Waite, Nanofiltration of natural organic matter: removal, fouling and the influence of multivalent ions, Desalination 118 (13) (1998) 109–122.
[14] L.H. Fan, J.L. Harris, F.A. Roddick, N.A. Booker, Influence of the characteristics of natural organic matter on the fouling of microfiltration membranes, Water Res. 35 (18) (2001) 4455–4463.
[15] M. Edwards, M.M. Benjamin, Transformation of NOM by ozone and its effect on iron and aluminum solubility, J. Am. Water Works Assoc. 84 (6) (1992) 56–66.
[16] A. Pihlajamäki, P. Väisänen, M. Nyström, Characterization of clean and fouled polymeric ultrafiltration membranes by Fourier transform IR spectroscopy-attenuated total reflection, Colloids Surf. A Physicochem. Eng. Aspects 138 (2–3) (1998) 323–333.
[17] C. Jucker, M.M. Clark, Adsorption of aquatic humic substances on hydrophobic ultrafiltration membranes, J. Membr. Sci. 97 (1994) 37–52.
[18] N. Her, G. Amy, C. Jarusutthirak, Seasonal variations of nanofiltration (NF) foulants: identification and control, Desalination 132 (1–3) (2000) 143–160.
[19] K.G. Linden, J.L. Darby, Ultraviolet disinfection of marginal effluents: ultraviolet absorbance and subsequent estimation of ultraviolet intensity, Water Environ. Res. 70 (2) (1998) 214–223.
[20] D. Belhateche, J.M. Symons, Using cobalt-ultraviolet spectrophotometry to measure hydrogen peroxide concentration in organically laden groundwaters, J. Am. Water Works Assoc. 83 (8) (1991) 23–30.
[21] I.M. Kolthoff, E.B. Sandell, E.J. Meehan, S. Bruckenstein, Quantitative Chemical Analysis, 4th ed., Permanganate, Cerium (IV), and Dichromate Methods, Macmillan, New York, 1969, Chapter 43, pp. 834–835, 1199.
[22] R.S. Summers, S.M. Hooper, H.M. Shukairy, G. Solarik, D. Owen, Assessing DBP yield: uniform formation conditions, Am. Water Works Assoc. J. 88 (6) (1996) 80–93.
[23] B.N. Badriyha, V. Ravindran, W. Den, M. Pirbazari, Bioadsorber efficiency, design, and performance forecasting for alachlor removal, Water Res. 37 (17) (2003) 4051–4072.
[24] Standard Methods for the Examination of Water and Wastewater, 20th ed., American Public Health Association, American Water Works Association, Water Pollution Control Federation, Washington, DC, 1998.
[25] P. Westerhoff, J. Debroux, G. Aiken, G. Amy, Ozone-induced changes in natural organic matter (NOM) structure, Ozone Sci. Eng. 21 (6) (1999) 551–570.
[26] M.S. Chandrakanth, G.L. Amy, Effects of NOM source variations and calcium complexation capacity on ozone-induced particle destabilization, Water Res. 32 (1) (1998) 115–124.
[27] W. Song, Nanofiltration of natural and synthetic organic chemicals with H_2O_2/UV pretreatment process, Ph.D. Thesis, Presented to the University of Southern California, Los Angeles, CA, 2003.
[28] A. Braghetta, F.A. DiGiano, W.P. Ball, Nanofiltration of natural organic matter: pH and ionic strength effects, J. Environ. Eng. 123 (7) (1997) 628–641.
[29] M.H. Tran-Ha, D.E. Wiley, The relationship between membrane cleaning efficiency and water quality, J. Membr. Sci. 145 (1) (1998) 99–110.
[30] S. Hong, M. Elimelech, Chemical and physical aspects of natural organic matter (NOM) fouling of nanofiltration membranes, J. Membr. Sci. 132 (2) (1997) 159–181.
[31] A. Braghetta, F.A. DiGiano, W.P. Ball, NOM accumulation at NF membrane surface: impact of chemistry and shear, J. Environ. Eng. 124 (11) (1998) 1087–1098.
[32] S. Belfer, J. Gilron, Y. Purinson, R. Fainshtain, N. Daltrophe, M. Priel, B. Tenzer, A. Toma, Effect of surface modification in preventing fouling of commercial swro membranes at the Eilat Seawater Desalination Pilot Plant, Desalination 139 (1–3) (2001) 169–176.
[33] D. Mukherjee, A. Kulkarni, W. Gill, Chemical treatment for improved performance of reverse osmosis membranes, Desalination 104 (3) (1996) 239–249.
[34] V. Lahoussine-Turcaud, M.R. Wiesner, J.Y. Bottero, Fouling in tangential-flow ultrafiltration: the effect of colloid size and coagulation pretreatment, J. Membr. Sci. 52 (1990) 229–237.